# An HPLC-SEC-based rapid quantification method for vesicular stomatitis virus particles to facilitate process development

Adrian Schimek,[1] Judy K.M. Ng,[1] Ioannes Basbas,[1] Fabian Martin,[1] Dongyue Xin,[2] David Saleh,[3] and Jürgen Hubbuch[4]

[1]ViraTherapeutics GmbH, Bundesstraße 27, 6063 Rum, Austria; [2]Boehringer Ingelheim Pharmaceuticals Inc, 900 Ridgebury Road, Ridgefield, CT 06877, USA; [3]Boehringer Ingelheim Pharma GmbH & Co. KG, Birkendorfer Str. 65, 88397 Biberach, Germany; [4]Karlsruhe Institute of Technology, Institute of Process Engineering in Life Sciences, Section IV Biomolecular Separation Engineering, Fritz-Haber-Weg 2, 76131 Karlsruhe, Germany

**Virus particle (VP) quantification plays a pivotal role in the development of production processes of VPs for virus-based therapies. The yield based on total VP count serves as a process performance indicator for evaluating process efficiency and consistency. Here, a label-free particle quantification method for enveloped VPs was developed, with potential applications in oncolytic virotherapy, vaccine development, and gene therapy. The method comprises size-exclusion chromatography (SEC) separation using high-performance liquid chromatography (HPLC) instruments. Ultraviolet (UV) was used for particle quantification and multi-angle light scattering (MALS) for particle characterization. Consistent recoveries of over 97% in the SEC were achieved upon mobile phase screenings and addition of bovine serum albumin (BSA) as sample stabilizer. A calibration curve was generated, and the method's performance and applicability to in-process samples were characterized. The assay's repeatability variation was <1% and its intermediate precision variation was <3%. The linear range of the method spans from $7.08 \times 10^8$ to $1.72 \times 10^{11}$ VP/mL, with a limit of detection (LOD) of $7.72 \times 10^7$ VP/mL and a lower limit of quantification (LLOQ) of $4.20 \times 10^8$ VP/mL. The method, characterized by its high precision, requires minimal hands-on time and provides same-day results, making it efficient for process development.**

## INTRODUCTION

Therapies based on virus particles (VPs) have significantly advanced over the past decades. Researchers have engineered and optimized VPs to expand their range of applications for various indications and also to enhance their safety and efficacy.[1] As a result, VP-based therapies are on their way to market with 331 active or recruiting clinical trials for gene therapies and 90 for oncolytic viruses, as listed by the US National Library of Medicine at the end of 2023.[2] For gene therapy, viruses are typically replication-incompetent and used as a vehicle to transfer genetic material to target cells. In contrast, oncolytic viruses are typically replication-competent in target cells and will multiply in the host.

Both enveloped and non-enveloped viruses are exploited for virus-based therapies. The surface of non-enveloped VPs is typically composed of a highly structured virus-encoded capsid shell consisting of multimers of protein subunits. Enveloped viruses, on the other hand, are enclosed with a lipid bilayer; its composition is directly dependent on the virus-encoded proteins, replication cycle, and host cell type. Thus, the surface of enveloped viruses is, in comparison, more complex and heterogeneous even within one production batch.

Despite the advancement of VP-based therapies, there remain significant challenges to develop manufacturing processes for such VPs. These challenges include the development of stable producer cell lines, the scalability of production, ensuring the purity and infectivity of the VPs, and maintaining the stability of the final product.[3–6] To address these challenges in process development, it is crucial to set up analytical tools to accurately quantify infectivity and particle concentration to determine yield after each step and evaluate the step and process performance.

Various quantification methods are widely used to measure different aspects of the target VPs, namely infectivity, genome copy, and particle quantification. Infectivity assays employ cell-based approaches to measure VPs that can successfully infect and replicate in host cells. Genome copy quantification is based on polymerase chain reaction (PCR) and will detect genetic material incorporated in both infectious and non-infectious VPs, as well as non-incorporated forms found in the sample. Particle quantification techniques based on physical measurement principles mostly rely on specialized devices such as nano particle tracking analysis (NTA), dynamic light scattering (DLS), tunable resistive pulse sensing (TRPS), and negative staining transmission electron microscopy (ns-TEM). A combination of some of

these techniques is necessary to properly describe the quality and quantity of VPs in a sample. Thus, VP analysis typically requires high laboratory workload, long analysis time, low sample throughput, and high result variability.[7–9] The lack of rapid at-line analytical methods to accurately characterize and quantify VPs is an issue faced in the development of viral therapies.[5] As the fields of gene therapies and oncolytic virus therapies continue to evolve, advancement of VP analytics will be essential for the successful development and commercialization.

Quantification methods based on ultraviolet (UV) detection of entire VPs have been published for several enveloped and non-enveloped particles.[10–15] All of the referenced quantification methods employ separation techniques (such as size-exclusion chromatography [SEC], ion-exchange chromatography [IEX], or capillary electrophoresis [CE]) that influence the analyte recovery and thereby the result. Reproducible recovery values that are within specified range were shown for non-enveloped viruses with all separation techniques, but not for enveloped viruses. SEC resin based on hydrophilic polymethacrylate has previously been shown to be suitable for virus analysis,[10,15,16] and it is hypothesized it may outperform IEX resins in terms of target recovery and shape preservation upon buffer optimization to maximize recovery. When the size difference between VPs and SEC resin pore size is sufficiently large, VPs are expected to elute in the void volume, which is seen on the chromatogram as the exclusion peak. Comparatively smaller protein impurities and nucleic acids will be retained longer in the resin and be therefore separated.

The enveloped virus used in this study is a modified vesicular stomatitis virus (VSV) of the Rhabdoviridae family. Rhabdoviruses are enveloped RNA viruses with a bullet-shaped morphology measuring $70 \times 196$ nm.[17,18] Though wild-type VSV already has versatile application potential as an oncolytic virus and vaccine vector,[19] further engineering of the virus by substitution of its glycoprotein (GP) for that from lymphocytic choriomeningitis virus (LCMV) has resulted in VSV-GP with minimal neurotoxicity, greater potency against human cancer cells, and escape from host humoral immunity.[20,21] Infectivity assays, such as 50% tissue culture infectious dose ($TCID_{50}$), plaque assay, and laser force cytology are available and used quantification methods for VSV and its variants.[22–24] Additionally, PCR and TRPS protocols have been established. However, these methods necessitate high laboratory workload and specialized machines, thus challenges in application remain.[22,25,26]

In this study, a straightforward method for total VP count for VSV-GP was developed. The key features of the method include low hands-on time, high precision, and same-day results. The working range for quantification was tailored to process development applications. To develop a robust, versatile, and sample matrix-independent method, a label-free approach was chosen. While the method is based on SEC separation and UV detection, a downstream in-line multi-angle light-scattering (MALS) detector provided additional particle characteristics such as particle size. Each component of the setup from sample preparation to the run method itself has been opti-

mized and characterized, and an example application for process development is presented. A standard curve based on purified reference virus material is used to interpolate absolute values. As an orthogonal method for sample characterization, ns-TEM was used as it is considered the established benchmark method for VP quantification for particle numbers.[8,27] High-performance liquid chromatography (HPLC) instruments equipped with UV detectors are ubiquitous in biopharmaceutical labs, and expertise and familiarity are typically well-established among researchers. This will facilitate wide implementation and applicability.

## RESULTS

### Reference material generation and characterization

Two batches of purified VSV-GP preparations were produced by sucrose cushion centrifugation followed by SEC. Both batches were analyzed using orthogonal quantification methods: ns-TEM, quantitative PCR (qPCR), and $TCID_{50}$ assay. The titers determined by ns-TEM were comparable between the two batches with $1.72 \times 10^{11}$ VP/mL for the first and $1.44 \times 10^{11}$ VP/mL for the second batch. The viral RNA in the sample was quantified by qPCR to be in the same magnitude as the ns-TEM, with $1.38 \times 10^{11}$ genomic copies per mL (GC/mL) for the first and $2.13 \times 10^{11}$ GC/mL for the second batch. Infectivity was confirmed by $TCID_{50}$ assay with $5.62 \times 10^{10}$ $TCID_{50}$/mL for the first and $3.06 \times 10^{10}$ $TCID_{50}$/mL for the second batch. The magnitude difference between genomic copies and infectivity is expected, as particle heterogeneity results in VPs that are unable to infect otherwise susceptible cells.[28]

### Analytical separation method on the HPLC

Virus preparations are injected into the HPLC-SEC setup with an in-line MALS detector and using an SEC resin that excludes VPs from entering the bead pores and thus separating them from smaller impurities. Separation of concentrated VSV-GP VPs from impurities is shown in Figure 1A, where a sample of purified VPs spiked with impurity-rich clarified harvest material was analyzed. The chromatogram can be divided into the distinct exclusion peak at 10.2 min and a second peak region eluting between 18 and 33 min. Separate injections in Figure 1B enable peak allocation, which shows the exclusion peak originates from the VSV-GP sample. The second peak region originates from the clarified harvest material. In the light-scattering signal only the exclusion peak is observed. This indicates large, thus scattering particles in the exclusion peak; and small, thus non-, or low-scattering particles for the second peak region. An analysis of the cell culture medium of the process revealed that the second peak region mostly originates from the cell culture media itself, except for the first eluting impurity peak. This first impurity peak was depleted upon nuclease-treatment, implying its nucleic acid content (data not shown).

### Virus peak identification

The presumed virus-containing exclusion peak, eluting at 10.2 min, was collected using a fraction collector, and analyzed by offline analytical methods to identify its VP identity. The presence of VPs in this fraction was confirmed by detection of viral genetic material by qPCR (showing a recovery of 63.3%) as well as by identifying virus-encoded
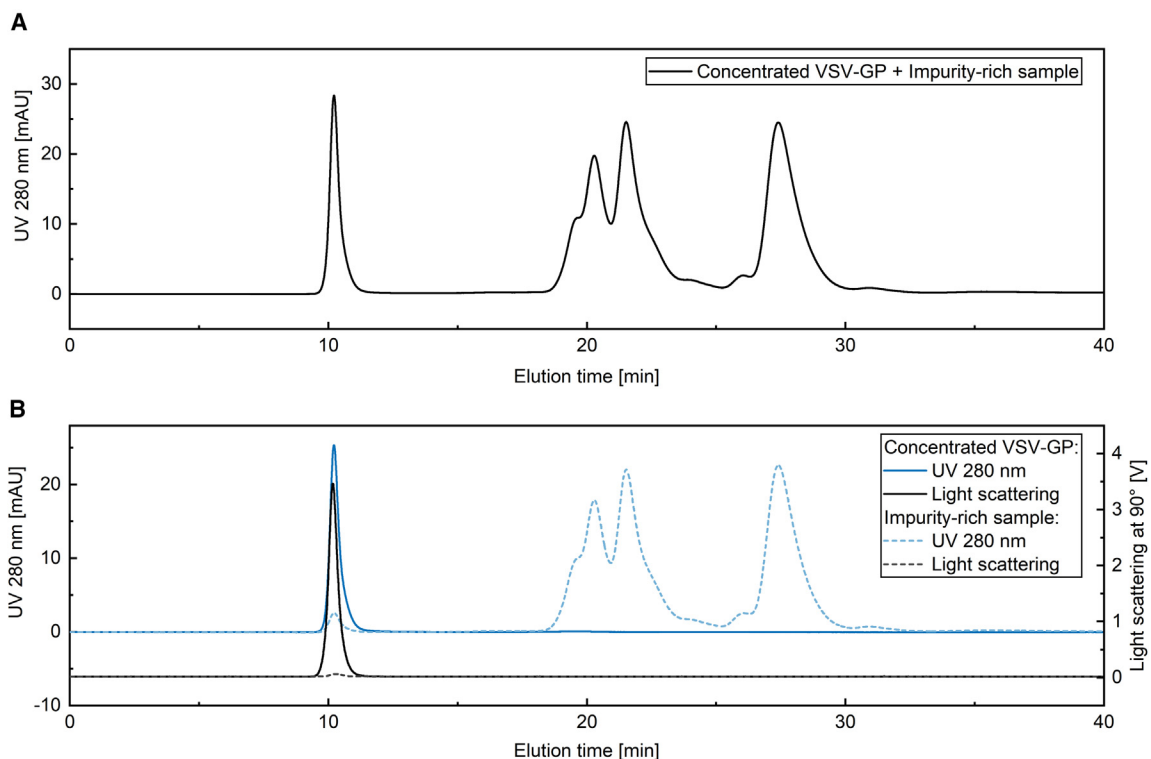
**Figure 1. SEC separation chromatogram of purified VSV-GP and impurity-rich material**

(A) Chromatogram of concentrated VSV-GP material (reference material) spiked into impurity-rich material (clarified harvest) on TSKgel G4000PW using optimized buffer conditions. (B) Concentrated VSV-GP material and impurity-rich material were injected separately on the SEC column using the same conditions. UV 280 nm and light-scattering signal at the 90° angle is shown.

protein bands using gel electrophoresis followed by silver staining as depicted in Figure S1 presented in the supplemental material.[28]

## Method development

The initial running buffer was a Tris-based buffer with 50 mM NaCl and 150 mM Arginine (Arg) at pH 7.5. Comparing the UV 280 nm signal responses of VSV-GP injections over the column and the bypass showed VSV-GP particle recovery values of about 30%. Also, the cleaning-in-place (CIP) steps showed particles eluting from the column that could be observed in the light-scattering signal (data not shown). Buffer screening was performed to increase recovery values by reduction of non-specific interaction of the analyte with the column. Simultaneously, two different pore sizes of the Tosoh TSKgel polymethacrylate resin (50 nm, >100 nm) and two column housing materials (stainless-steel, polyetheretherketone [PEEK]) were tested for resolution improvement and sample recovery. Sample stability issues were addressed by spiking of BSA (bovine serum albumin) as a stabilizer to the samples. The aim was to increase storage duration in the system sample manager until the sample injection for analysis was performed.

## Mobile phase buffer screening

Buffer screenings were performed to minimize non-specific binding of the VPs to the column resin, which are mainly due to a combination of hydrophobic and electrostatic interactions.[29] Following each buffer optimization run, two CIP steps (organic solvent and high-salt buffer) were conducted with the aim of specifically eluting bound VPs based on their interaction type. During these CIP steps, the MALS signal was qualitatively assessed to determine the residual interaction type prevailing by the buffer used.

The mobile phase was optimized in seven iteration rounds of buffer screening, each consisting of multiple runs. In each round, the buffers were adjusted based on the recovery and CIP results from the previous rounds and literature research. A detailed buffer list can be found in Table S1, the iteration rounds consisted of the following:

(I) Tris-based buffer with increasing salt content
(II) Tris-based buffer with Arginine and pH adjustments
(III) Citrate and phosphate-based buffer testing
(IV) Tris-based buffer with combined Arginine and salt content adjustment
(V) Tris-based buffer with additives (sorbitol, sucrose, dimethyl sulfoxide [DMSO])
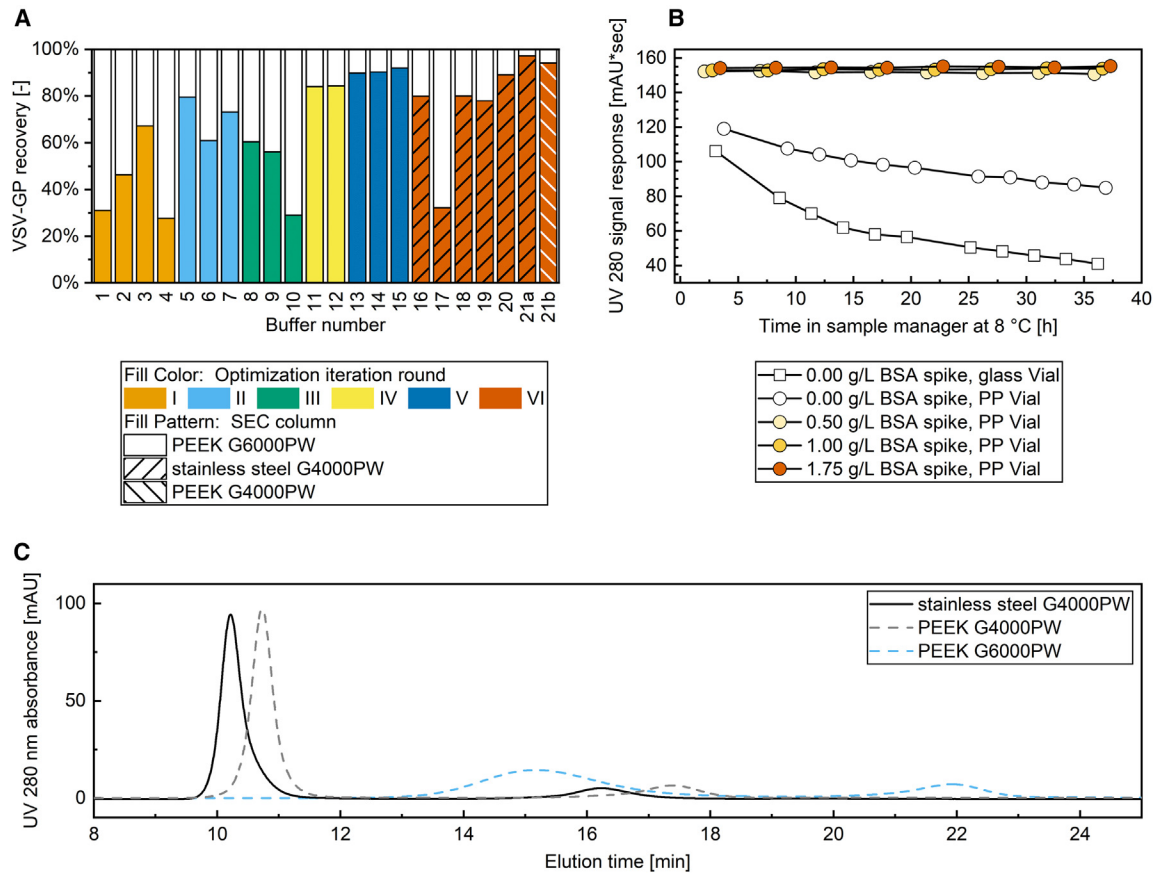(VI) Tris-based buffer with Arginine, salt, and DMSO content adjustments

**Figure 2. Buffer screening, sample stability testing, and analytical SEC column selection for method development**

(A) Recovery values for virus particles upon the mobile phase optimization. Iteration rounds: I – Tris-based buffer with increasing salt content, II – Tris-based buffer with Arg and pH adjustments, III – Citrate- and phosphate-based buffer testing, IV – Tris-based buffer with combined Arg and salt content adjustment, V – Tris-based buffer with additives (sorbitol, sucrose, DMSO), VI – Tris-based buffer with Arg, salt, and DMSO content adjustments; technical replicates: $n = 1$ for buffers 1 to 20, $n = 3$ for buffer 21 (SD < 0.8%). (B) Sample stability optimization using different vials (glass and polypropylene vials) and BSA spiking. The UV 280 nm signal response is the integrated exclusion peak, identified as the virus peak. (C) SEC chromatogram comparison of BSA-spiked reference material for stainless-steel and PEEK version of G4000PW and PEEK version of G6000PW.

The initial low recovery using a non-optimized buffer could be improved by adjusting the salt and Arg content of the Tris-based buffer. A sample recovery of 84.4% could be reached after two iteration rounds as depicted in Figure 2A. The use of phosphate-based buffers and citrate as an additive did not improve recoveries. Sorbitol, sucrose, and DMSO increased recoveries, from which DMSO performed best under the tested conditions. The overall best performance of this system was achieved using a buffer composed of 50 mM Tris, 200 mM NaCl, 150 mM Arg, and 0.1% DMSO at pH 8.0: A recovery of 97.2% (SD 0.54%) on the stainless-steel version of G4000PW was reached and 94.2% (SD 0.76%) on the PEEK version. Simultaneous to the buffer screening with VSV-GP, the recoveries for BSA were determined. In the iteration rounds 1 to 4, the recovery values for BSA were much higher compared with VSV-GP with values above 70%, averaging at 87.4%. For the final buffer (number 21 Figure 2A), a BSA recovery of 96.88% (SD 0.56%) was reached for the stainless-steel version

and 97.24% (SD 0.56%) for the PEEK version. (BSA recovery data not shown).

### Sample stability optimization

A decrease in UV 280 nm signal response over time was observed for VSV-GP samples stored in the sample manager. This was likely due to non-specific adsorption of purified VPs to storage material surfaces. To address this issue, two different HPLC sample vial materials (glass and polypropylene [PP]) were tested as well as BSA spiking of the samples. Prior to BSA spiking, the reference material was diluted to a concentration of $9 \times 10^9$ VP/mL. Prepared samples were stored in the sample manager at 8°C over a time frame of 35 h and the signal response repeatedly determined. The results are depicted in Figure 2B. The first time point for non-spiked samples in the glass vial and the polypropylene vial resulted in 70% to 80% signal responses in comparison to the BSA-spiked sample. Over the course of the measurement, the signal response for the non-spiked samples further
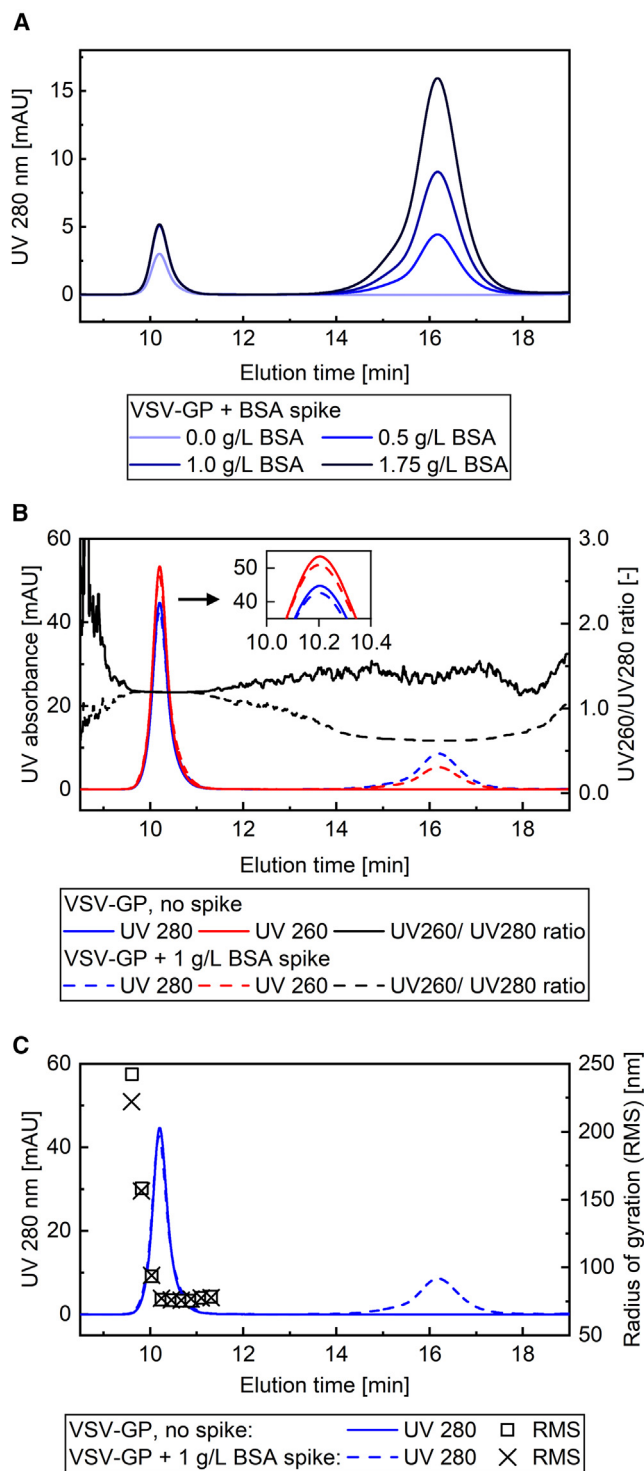
**Figure 3. Exclusion peak characterization using BSA as sample stabilizer**
(A) SEC chromatogram of reference material spiked with different concentrations of BSA and non-spiked. The exclusion peaks at 10.2 min of the BSA-spiked samples are entirely overlaying. The non-spiked sample has been in the sample manager for several hours before measurement. (B) UV 260 nm and UV 280 nm absorbance for

decreased to 57% for the polypropylene vial and 28% for the glass vial. The UV 280-nm signal response for samples with BSA spikes were stable over the complete time frame with an RSD below 0.5%.

### Column comparison

Two different pore sizes of the Tosoh TSKgel PW resin (G6000PW and G4000PW) were compared for resolution, and additionally two different column housing materials were tested for recovery. The specified mean pore sizes for the resins are 50 nm for the G4000PW and >100 nm for the G6000PW. Upon comparison of the exclusion peaks of the different columns in Figure 2C, differences in elution time and widths are observed. The PEEK G6000PW column resulted in later (4 to 4.5 min) and broader peaks (by the factor 3.3) compared with the G4000PW columns. The time shift and especially the broad peak indicates a greater retention of the VPs by the greater pore sizes. It is assumed the G6000PW resin pores are, at least partially, large enough to retard VPs, in contrast to the G4000PW resin pores that predominantly exclude them. The PEEK column housing has an inner diameter of 7.8 mm compared with 7.5 mm for the standard stainless-steel housing that results in an increased column volume of 8.2%. The PEEK version of the G4000PW retards the elution time for 31 s compared with the stainless-steel version. However, the peak shape remains comparable between the column housings.

BSA was used as sample stabilizer, and it can also be seen as a model impurity protein for column comparison as shown in Figure 2C. As expected, the BSA spike peaks elute after a longer retention time compared to the VPs. They are broadened in a similar way as the VP peaks in respective to the column used. However, the use of the G6000PW resin leads to a reduced separation efficiency without distinct baseline separation. Together with the recovery results, it was decided to continue method development using the stainless-steel version of the G4000PW.

### Separation characterization using BSA as sample stabilizer

The online signals of the UV and MALS detectors were used to characterize the obtained chromatograms, focusing on the exclusion peaks. In the method setup, BSA was spiked into the samples as a stabilizing agent. Chromatograms of BSA-spiked and non-spiked reference material are shown in Figures 3. Injecting the reference VP material into the analytical SEC column results in a single peak at an elution time of 10.2 min. Different BSA spiking concentrations (0.5 to 1.75 g/L) were used in Figure 3A, resulting in a later eluting BSA peak without any effect on the elution behavior of the exclusion peak. A reduced peak area for the non-spiked sample was observed after several hours in the sample manager before injection, indicating some loss of sample during prolonged storage without addition of

non-spiked and BSA-spiked reference material and UV260/280 nm ratio; a percentile filter of 50 was used to smooth the ratio curve. (C) RMS-radii for non-spiked and BSA-spiked reference material. Radii were only evaluable for the exclusion peak due to the low light-scattering signal for the rest of the chromatogram.
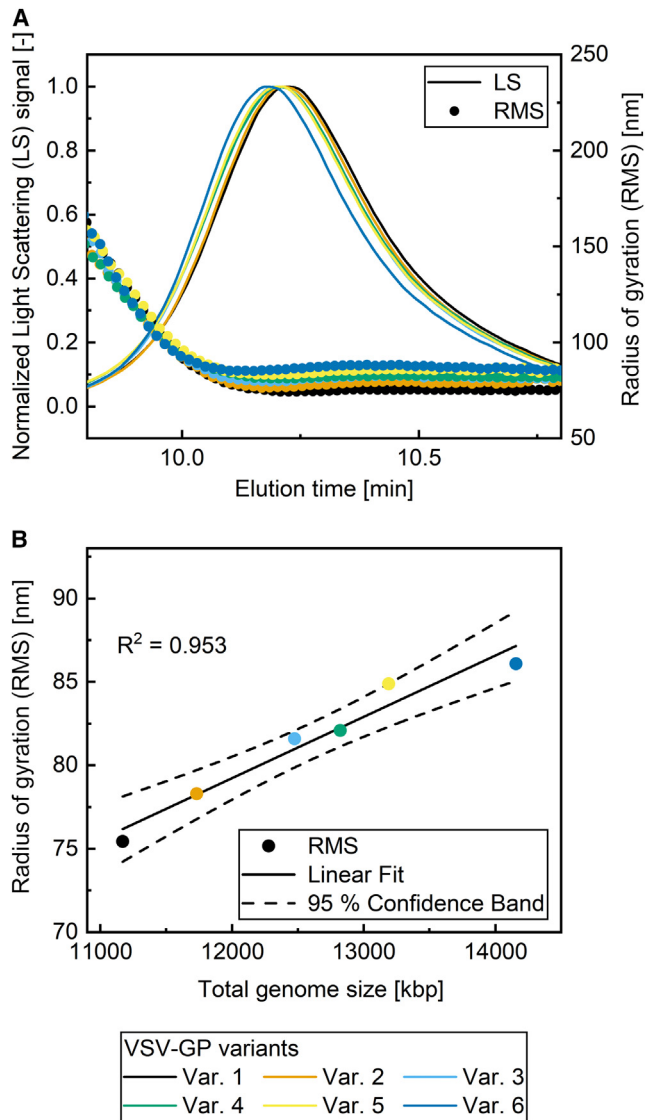
**Figure 4. VP size influence on the exclusion peak and VP sizing**
(A) SEC exclusion peak of VSV-GP and variants of different genome sizes. Normalized light scattering and radius of gyration. (B) Radius of gyration for VSV-GP (Variant 1) and larger size variants (Variants 2 to 6) over variant genome size. The radii were measured at the peak maximum of the exclusion peak.

BSA as stabilizer. The ratio of UV 260 nm to UV 280 nm results in a value of 1.196 (SD 0.004) for the first elution peak at 10.2 min as depicted in Figure 3B. The difference of the ratios between the BSA-spiked and non-spiked measurement lays within the standard deviation. With the addition of BSA, a second peak is observed in the UV signal at a later elution time point (16.2 min). At its peak maximum, a ratio of UV 260 nm to UV 280 nm of 0.624 is reached. In Figure 3C, size measurements based on the online light-scattering signal results in a radius of gyration of 76.4 nm (SD 0.6) for the constant region after peak fronting. The size difference between the BSA-spiked and non-spiked measurement lies within the standard deviation. In the

front of the peak, larger radii are measured, with a maximum of approximately 250 nm.

*Virus size variants*
Virus preparations of VSV-GP variants with different total genome sizes were analyzed, and their particle sizes measured using the MALS detector signal. A shift of less than 2 s in maximum of the exclusion peak to an earlier elution time point with increasing genome size is shown in Figure 4A. The measured size of the peak maximum is plotted over the total genome size in Figure 4B. A linear regression shows the linear dependency of particle size and total genome size.

*Calibration curve for VP quantification*
A dilution series of the reference material containing purified VPs was analyzed by HPLC-SEC and is shown in Figure 5A. No difference in elution time and general peak shape is observed. Both online and offline analysis indicated no interference for the exclusion peak by other particles than the VPs and showed a baseline separation from smaller impurities. The reference material and the developed SEC method are deemed suitable for generating a calibration curve. The UV 280 nm signal response was defined as the integrated peak area of the exclusion peak at 10.2 min, identified as the virus peak. The signal responses of eight concentration levels of the reference material were plotted to obtain the calibration curve shown in Figure 5B. The linear regression was 1/Y-weighted due to the heteroscedasticity of the dataset and forced through the origin. The dependency of the response to the VP concentration in the sample is given by Equation 1, where $y$ is the signal response in mAU * sec and $x$ is the VP concentration in VP/mL. The coefficient of determination was calculated as $R^2 = 0.998$. The concentration range of the calibration curve reaches from $7.08 \times 10^8$ to $1.72 \times 10^{11}$ VP/mL.

$$y = 1.5503 * 10^{-8} \frac{\mathrm{mAU} * \sec}{\mathrm{VP/mL}} * x \qquad \text{(Equation 1)}$$

**Method characterization**
*Performance*
The performance of the method was tested at four concentration levels within the working range with the lowest being the lower limit of quantification (LLOQ). Based on the signal-to-noise (SN) ratio, the theoretical sensitivity of the method was calculated. A ratio of 3 was applied for the limit of detection (LOD) and a ratio of 10 for the LLOQ, resulting in an LOD = $7.72 \times 10^7$ VP/mL and an LLOQ = $2.57 \times 10^8$ VP/mL. However, sufficient accuracy was only reached for an LLOQ of $4.20 \times 10^8$ VP/mL, which was used for the performance evaluation. Accuracy, repeatability, and intermediated precision have been determined and are shown in Table 1. Recommended specifications by the Food and Drug Administration (FDA) guidelines were met or exceeded.[30]

*Sample matrix influence*
The influence of different sample matrices on the VP recovery was evaluated. In early downstream process (DSP) steps, the process
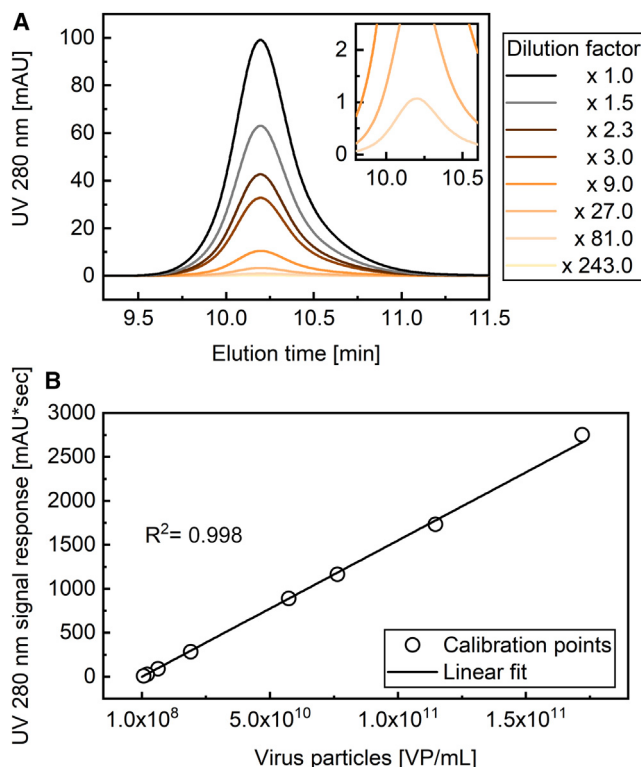
**Figure 5. Calibration curve**

Diluted reference material was analyzed using BSA as the sample stabilizer to obtain measurement points for the calibration curve. The UV 280 nm integrated area of the exclusion peaks was used as signal response. Three independent runs in triplicate for eight concentration levels were obtained. (A) Exemplary exclusion peaks of the concentration levels used for the calibration are shown in comparison. (B) A 1/Y-weighted linear regression was used to fit calibration curve. Only mean values are shown due to non-displayable RSD <2% and for the lowest concentration RSD <4.5%.

material matrix consists of spent cell culture media and cell-derived impurities. Nuclease is added to degrade host cell DNA and RNA. DNA and RNA fragments, as well as other residual impurities are removed throughout the process steps. Buffer compositions are changing along the process, and the total salt concentration varies and can go up to a maximum of 1 M.

For VSV-GP, cell culture media is replaced by Tris-based buffers early in the DSP and formulated with excipients such as albumin and trehalose. To examine the influence of the process sample matrices on the quantification method, samples were generated for analysis with the following method: in-process control samples from each step were filtered to deplete the VPs they originally contain, and then a defined amount of VP was spiked into each sample. The samples were first checked by HPLC-SEC (<LOD) for successful VP removal prior to spiking. The results, as presented in Table 2, show an average accuracy of 99.79% for all in-process controls (IPCs) with a standard deviation of 5.64%, indicating that the quantification method is not influenced by the sample matrices tested.

## Chromatographic step mass balance

Utility of the quantification method described in this paper was demonstrated through performance of a mass balance calculation of a typical chromatographic capture step. VSV-GP was propagated in cell culture, and the conditioned clarified harvest material fed into a cation exchange chromatography (CEX) monolith column in bind-and-elute mode. VP concentration of the input feed and output flowthrough, wash, and elution were quantified by HPLC-SEC method. Fractions with expected high concentrations of VSV-GP were diluted (10× or 100×) so that the concentrations fall within the calibrated range of the method. Collected output fractions were analyzed by qPCR in parallel.

The online chromatogram signals are shown in Figure 6A and the offline fraction analysis results in Figure 6B. One liter of feed with a concentration of $2.39 \times 10^9$ VP/mL was loaded on the column, and a total of $2.76 \times 10^{12}$ VPs were quantified by the HPLC-SEC method in the output fractions. Specifically, 18.8% of the total VPs in the feed was measured in the column flowthrough, VP concentration in the column wash was below LLOQ, and 66.3% was detected in the main peak with a peak width of 1.6 mL. The entire elution peak including the tailing was 9.8 mL wide and 78.8% of total input VPs was found. Additionally, the CIP peak was pH-stabilized and also collected for quantification, showing a result of 2.4% of total VPs. Overall, the total VPs quantified in the output is marginally higher than the expected total particle counts in the feed and falls within the accepted error margin of the performance runs.

The quantification results obtained from the presented HPLC-SEC method and from the established qPCR method were comparable: feed concentration $2.8 \times 10^8$ GC/mL, $5.0 \times 10^8$ VP/mL; elution peak particle count $2.03 \times 10^{12}$ GC, $2.1 \times 10^{12}$ VP.

## DISCUSSION

### Separation method and method development

In-process control samples generated from process development and production of VPs vary in buffer composition, particle concentration, and amount of process-related impurities.[31] UV-absorbing impurities need to be depleted or shown to be of neglectable concentration before target quantification by UV, thus framing the separation problem to be solved prior to the quantification. Another challenge is maintaining the integrity of the viral particles during the analytical method; all system parameters, including flow rate and resin bead size, were selected to minimize shear forces incurred. Such system parameters, once selected, remained unchanged during method development in this study.

The exclusion peak was identified as the virus peak by offline analytical methods as well as by characterization using online detectors. The online UV data show a constant ratio of UV 260 nm to UV 280 nm ratio of 1.2 over the width of the exclusion peak, indicating the presence of nucleic acids and proteins at the same time, though no more information about the sample composition can be derived. However, the consistency of the obtained value leads to the conclusion of a

**Table 1. Performance evaluation**

| Level | Expected titer [VP/mL] | Mean [VP/mL] | Standard Dev. [VP/mL] | 95% confidence interval [VP/mL] | Accuracy | Repeatability RSD | Intermediate precision RSD |
|---|---|---|---|---|---|---|---|
| H | $1.44 \times 10^{11}$ | $1.64 \times 10^{11}$ | $6.31 \times 10^{8}$ | $1.63 \times 10^{11}$ to $1.64 \times 10^{11}$ | 113.7% | 0.63% | 0.75% |
| M | $2.06 \times 10^{10}$ | $2.19 \times 10^{10}$ | $1.88 \times 10^{8}$ | $2.17 \times 10^{10}$ to $2.21 \times 10^{10}$ | 106.2% | 0.09% | 1.67% |
| L | $2.94 \times 10^{9}$ | $2.97 \times 10^{9}$ | $3.28 \times 10^{7}$ | $2.93 \times 10^{9}$ to $3.00 \times 10^{9}$ | 100.9% | 0.59% | 2.14% |
| LLOQ | $4.20 \times 10^{8}$ | $4.23 \times 10^{8}$ | $6.44 \times 10^{6}$ | $4.15 \times 10^{8}$ to $4.30 \times 10^{8}$ | 100.6% | 0.49% | 2.95% |

Four concentration levels (High [H], Middle [M], Low [L], and LLOQ) were used to evaluate the performance of the HPLC-SEC quantification. For the concentration levels, reference material was diluted, aliquoted and stored at $-80°C$ until usage. Measurements were done in triplicate in five independent runs.

constant ratio of nucleic acid to protein content over the width of the exclusion peak. Furthermore, it indicates no increase or decrease in light-scattering effects over the peak.[32] The in-line MALS detector can show the presence of particles in the expected size range for the target VPs. The sizing data of the MALS also reveals the presence of larger particles in the beginning of the exclusion peak with radii up to 250 nm for the start of the peak, and then constant sizes are measured throughout the rest of the exclusion peak. The larger particles eluting first may be VP aggregates still showing an unaltered UV 260 nm to UV 280 nm ratio. This observation indicates a weak separation effect of the SEC column at particle sizes much larger than its specified pore sizes, possibly induced by a broad pore size range of the SEC column or, as suspected by Vajda et al., a separation effect of the inter-particle volume.[33] This effect can also be observed when comparing the exclusion peak time points of virus variants varying in particle size. The increased particle length correlates with shift toward an earlier elution. The correlation seen with the observed separation effects and sizing data to the theoretical VP sizes indicates that the integrity of the VPs is preserved in this analytical method.

For the method characterization runs, purified VP preparations defined as reference material were used. The material was purified and concentrated by sucrose cushion centrifugation and polished using preparative SEC. However, possible impurities of similar size and density range as the VPs cannot be depleted by these steps. From analysis of previous established methods (qPCR and ns-TEM), as well as

considering the lack of UV-signal and light-scattering interference signals, the preparations were deemed suitable for use as a VP standard. Similar observations for the exclusion peak in the online signal are made for IPC samples, making the peak suitable to be used for quantification purposes. A dilution series of the reference material was used to obtain a calibration curve based on the UV 280 nm signal response. The calibration curve showed good linearity in the examined range. While this approach requires an orthogonal quantified reference material, it does not require knowledge of target molecule or solute-specific optical parameters in comparison with methods based on light-scattering principles.[34]

To increase the sample recovery of the SEC method, the running buffer was optimized using a buffer screening. The rationale was to reduce suspected hydrophobic and electrostatic interactions with the column resin when altering the buffer composition. The low initial recovery could be improved by shielding electrostatic interactions by increasing the NaCl concentration until the point where the salt enhanced hydrophobic interactions leading again to a reduced recovery. Arginine proved to be a good agent to suppress both interactions as previously reported.[35] Observed recoveries for BSA were higher compared with VSV-GP for the first four iteration rounds, indicating additional or stronger interactions of the much larger VPs with the resin. Addition of sugars and organic solvents increased the recovery for VPs, of which DMSO performed best. DMSO was reported to stabilize enveloped VPs during freeze-thaw cycles,[36] but

**Table 2. Results of the sample matrix influence evaluation**

| | IPC 1 | IPC 2 | IPC 3 | IPC 4 | IPC 5 | IPC 6 |
|---|---|---|---|---|---|---|
| Mean | $3.56 \times 10^{10}$ | $3.58 \times 10^{10}$ | $3.19 \times 10^{10}$ | $3.58 \times 10^{10}$ | $3.56 \times 10^{10}$ | $3.13 \times 10^{10}$ |
| Standard deviation | $5.41 \times 10^{7}$ | $8.24 \times 10^{7}$ | $7.98 \times 10^{8}$ | $5.46 \times 10^{6}$ | $8.81 \times 10^{7}$ | $4.95 \times 10^{8}$ |
| RSD | 0.15% | 0.23% | 2.50% | 0.02% | 0.25% | 1.58% |
| 95% confidence interval | $3.55 \times 10^{10}$ to $3.57 \times 10^{10}$ | $3.57 \times 10^{10}$ to $3.59 \times 10^{10}$ | $3.10 \times 10^{10}$ to $3.28 \times 10^{10}$ | $3.58 \times 10^{10}$ to $3.58 \times 10^{10}$ | $3.56 \times 10^{10}$ to $3.58 \times 10^{10}$ | $3.08 \times 10^{10}$ to $3.19 \times 10^{10}$ |
| Accuracy | 103.4% | 104.0% | 92.7% | 104.0% | 103.6% | 91.0% |

IPCs of a lab-scale production run were taken, the virus particles removed by filtration, and a specified virus concentration spiked in. Samples were measured in triplicate by HPLC-SEC quantification. The spike concentration in the sample was $3.44 \times 10^{10}$ VP/mL. Purification stage and differences between IPCs are as follows. IPC 1: harvested cell culture including cell culture media, increased ionic strength for viral release, clarified by depth filtration; IPC 2: nuclease treated clarified harvested material; IPC 3: CEX purified material, CEX eluate consists of a Tris-based buffer containing Arginine and NaCl; IPC 4: polished material with reduced impurity content; IPC 5: buffer exchanged to a Tris-based buffer containing Arginine and excipients; IPC 6: material spiked with additives.
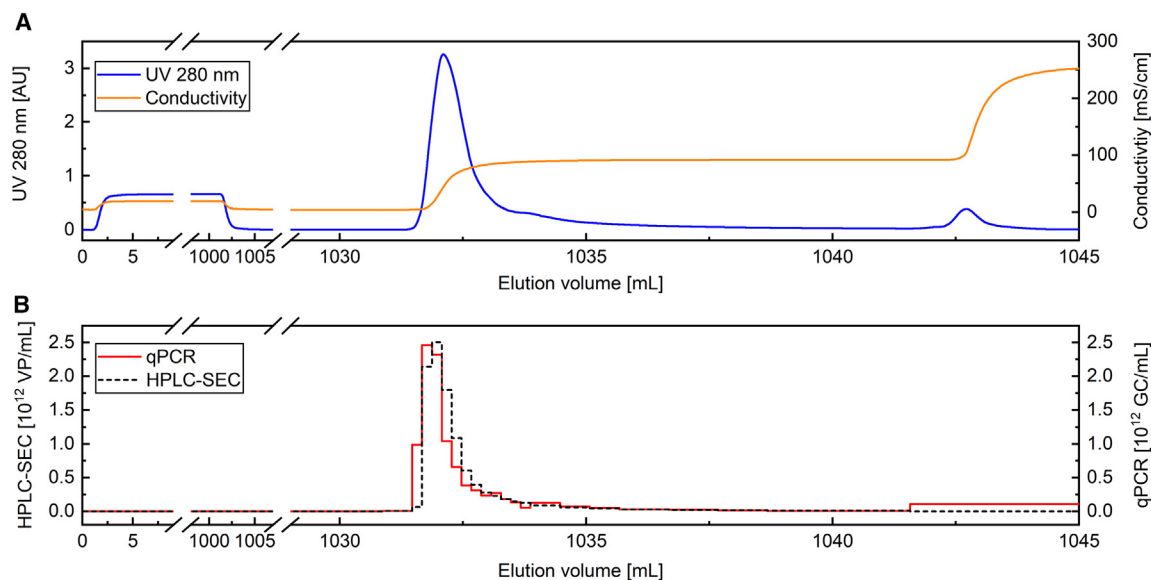
**Figure 6. Offline fraction VP quantification of a CEX purification step**

Clarified harvest material of a VSV-GP upstream process was applied in bind-and-elute mode on a CEX monolith column. Fractions of load, wash, elution, and CIP were collected and quantified offline by the presented HPLC-SEC method and qPCR. (A) Chromatogram of CEX run showing online UV 280 nm signal and online conductivity signal. The UV signal saturated at 3.0 AU. (B) Fraction quantification results for HPLC-SEC and qPCR. Due to low numbers for the load phase (and CIP for HPLC-SEC) and scale limitations, signals are plotted close to zero for these phases.

could also have a negative effect on VP integrity due to increased lipid bilayer permeability.[37] Thus, DMSO was reduced from 1% in first screening runs to 0.1% without impacting recovery values. For quantification purposes, a sufficiently high recovery is required, though it does not have to be 100% as stated by an FDA guideline.[30] Rather, the recovery values should be consistent and reproducible. Within the buffer screening, the final buffer was tested in triplicates with recovery RSDs below 0.6% for VSV-GP and BSA samples. The VSV-GP recoveries were later validated for four concentration levels in the performance evaluation.

Spiking BSA into the sample to act as a stabilizer enabled overnight measurements. Without BSA, UV 280 nm signal response was reduced by as much as 70% after 35 h in the temperature-controlled sample manager module. To explain and overcome this sample loss, different theories are considered. Aggregated VPs, retained by the column frit, would accumulate over injection count, leading to increased system pressure. Degraded VPs, disintegrated to fragments of smaller size, would be separated in the SEC column from the exclusion peak. However, such effects were not observed. It was thus hypothesized that VP adhered to the HPLC vial walls. To assess this hypothesis, the available wall area per VP was estimated. For 100 μL sample fill volume in the vials, the contact surface was calculated. As no technical drawings or vial interior dimensions were available, manual length measurements and surface calculations for cylinders and cones were used as geometrical approximations. A contact surface of 115 mm$^2$ was estimated for the glass vial, resp. 228 mm$^2$ for the polypropylene vial. Based on the VSV particle dimensions by Ge et al.,[17]

the projected sideways rectangle for a single VP was calculated to be $1.4 \times 10^{-8}$ mm$^2$. Based on the virus concentration in the sample and the signal reduction between the non-spiked samples and the spiked samples, the amount of presumed non-detected VPs was calculated. At the last time point of the sample stability experiment, each non-detected VP had 1.3, resp. 2.11 times more area available than its own projection on the surface. This estimation confirms the possibility of a Langmuir layer adhesion of the particles in terms of available wall area per particle. Furthermore, the declining VP concentration curves without BSA spikes observed in Figure 2B correspond to a Langmuirian adsorption kinetic.[38] The subsequent use of polypropylene vials coated with a high-performance surface did improve the sample stability but was not sufficient to enable a constant overnight signal response. BSA was reported to prevent non-specific sample binding on vial walls and the spiking of BSA to VSV-GP samples stabilized the resulting UV 280 nm response over the tested time frame of 35 h.[39] BSA spiking concentrations over the range of 0.5 to 1.75 g/L showed similar results without influencing the elution behavior of VPs or changing the rms radius. The results are in agreement with a published HPLC method development by Lorbetskie et al. in which the change from glass to polypropylene vials improved the recovery, however only the addition of an additive to the sample yielded in the sufficient reproducibility.[40]

Non-specific binding losses to HPLC vials were targeted using BSA as the sample stabilizer. Further losses could occur in other parts of the HPLC system such as the measurement chambers, tubings and connectors. These losses were minimized by the use of the "Bio" version

of the HPLC system which features bio-compatible materials for the wetted parts of the flow path up to and including the UV detector. Furthermore, the column resin and housing can induce non-specific binding. The column resin material was chosen according to manufacturer's information regarding suitability for VPs and already published applications for VPs.[10,15,16] After the above-described buffer optimization, a reproducible and high recovery of VPs from the column was achieved, showing neglectable residual interactions. Also, the column housing material was evaluated for sample recovery. Because the stainless-steel column showed high recovery and faster elution times compared with the PEEK housing, it was chosen for further method development. In case of the TSKgel G6000PW resin, the manufacturer's data of the pore size is vague with a size specification of >100 nm and the resin material has shown to produce a broad pore size distribution.[33] Diffusion effects and pore accessibility for the bullet-shaped VSV particles depend on their orientation, resulting in different possible retention behaviors for the same particle. Predominant retention effects due to pore accessibility is seen only with the G6000PW resin, resulting in a broader peak compared with the G4000PW resin with a specified mean pore size of 50 nm. However, a weak separation effect by size is also observed for the G4000PW resin. Baseline separation from protein impurities, shown for BSA as model impurity, was only achieved using the G4000PW resin, independent of the column housing.

### Method characterization

The performance evaluation based on four concentration levels showed a high reproducibility and intermediate precision for all tested levels. Accuracy values decreased with increasing VP concentration. For the highest level, 13.7% deviation was observed, which is still within the FDA recommended specification of 15%, but close to the threshold.[30] Highly concentrated samples should thus be diluted for increased accuracy and extrapolation to higher levels should be omitted. This is an assumption as higher concentration levels were not tested due to the lack of well-characterized and highly concentrated material, which limited the exploration range. Theoretical sensitivity values were calculated based on the SN ratio. In order to meet performance expectations, an LLOQ concentration between the theoretical value and the lowest calibration value had to be chosen. The LLOQ measurement point, extrapolated from the calibration curve, showed good results in the method performance evaluation. It led to an established working range across 2.5 orders of magnitude from $4.20 \times 10^8$ to $1.44 \times 10^{11}$ VP/mL. This range is at the upper end of published measurement ranges of other HPLC-based quantification methods for enveloped VPs.[11,13–15,41] The method's sensitivity is similar or better than the referenced quantification methods, which are all label-free methods. The use of signal-enhancing labeling dyes can increase sensitivities without reducing the measurement range.[42,43] Transfiguracion and colleagues used a fluorophore to stain viral nucleic acids without the need for VP lysis or membrane permeabilization. The labeling method reached seven times lower LLOQ compared with the herein presented method.[43] However, to develop a robust and versatile method, as well as to minimize the method's complexity, no signal enhancers were used. At the same time this approach maximizes sample recovery and reduces the probability of errors by preparational steps, thus minimizing the method's variability. A possible approach to improve the sensitivity limitation of the method is the increase of injected sample volume of currently 10 μL.

Samples from six production process steps, representing the major matrix changes in the DSP process have been analyzed to ascertain the robustness of the method in response to variations in sample matrices. Results showed a low variance (<2.5%) and an averaged accuracy of 99.79%. Sample matrix components were separated from the VPs and diluted in the SEC column, thus the matrix effect on the recovery and accuracy was low. BSA spiking seems to prevent VP adsorption in all tested sample matrices as the largest signal reductions were still below 10%.

### Chromatographic step mass balance

The main objective of the developed method was a straightforward, rapid, and robust quantification method for analyzing process development samples of VSV-GP particles. This method facilitated the characterization of a chromatography run based on the collected fractions. The mass balance application shows a sufficient precision to allocate VP percentages to chromatography phases. Results were obtained the following day, due to an overnight (12 h) sample throughput for 20 samples. The results for a single sample can be determined within 1 h, enabling the immediate at-line determination of the step yield, if required. The availability of this process performance indicator enables same-day process decisions beneficial in process development. Results were confirmed by qPCR analysis, which shows comparable counts for the eluted peak. In the SEC chromatogram, the virus peak elutes in the first half and later peaks are neglected for VP quantification purposes. Consequently, a tandem column setup could be employed in order to interlace subsequent analysis runs and increase the sample throughput without altering the flow rate or the column size.[44] In the current method setup, there is broad elution time gap between the exclusion peak and the impurity peak. Thus, another approach to reduce the analysis time could be the use of a shorter SEC column. If required, smaller resin beads could improve separation efficiency in shorter columns. However, smaller beads increase backpressure and thus the shear stress on VPs, which may damage the VPs.

### Summary

A robust method with rapid turnaround time for the quantification of VSV-GP particles was presented. Performance evaluation and a mass balance example using harvest material on a CEX column shows the applicability for IPCs and use for DSP process development. Absolute quantification relies on a reference VP material that was quantified by an orthogonal method; however, relative quantification can be performed in the absence of such reference material. The method was specifically established for enveloped viruses being generally more challenging in terms of physico-chemical properties and stability. The applicability to other VPs or variants of oncolytic viruses or gene therapies has yet to be shown, though it is assumed to be feasible with the suitable SEC pore size. The required knowledge about the

VPs is low and devices used are ubiquitous in biopharmaceutical laboratories. The MALS detector proved to be a useful tool for method development and can size particles, but the method application does not rely on it. For process development, the method allows determination of particle titers on the same day, enabling mass balancing and faster process decisions in the lab. Alternative methods such as PCR (qPCR or digital PCR) and $TCID_{50}$ remain essential because the additional information about genomic copies and infectious titers is beyond the scope of this method. For virus samples, multiple assays are typically required to gain the full picture of its composition and virus quality.

## MATERIALS AND METHODS

### Virus preparation

To generate VSV-GP, VPs were propagated by infection in mammalian cell suspension. Upon harvest at 34 h after infection, the suspension was treated with 200 mM NaCl. The harvest was clarified by centrifugation (5 min, $2\,000 \times g$), filtered (0.22 µm), and then treated with nuclease. A Tris-based buffer with NaCl and 150 mM Arg at a pH of 7.5 was used in all subsequent steps. The virus-containing material was underlaid by a 20 w/v-% sucrose cushion and centrifuged at 6°C for 14 h at 5 000 rpm. The resulting pellet was resuspended and filtered (0.22 µm). A preparative SEC column comprising Sepharose 6FF (Cytiva, Marlborough, MA, USA) was used for polishing of the material. The final virus suspension was sterile-filtered (0.22 µm), aliquoted, and stored at −80°C until usage. Two batches were used for experiments to optimize and characterize the method.

For further method characterization, material generated from a different lab-scale production process was used. The upstream process (USP) is as described above, and the DSP involves an IEX step and further filtration steps as described in the process patent application.[45]

### Generation of virus variants

Virus variants with varying genomic sizes were generated using the Gibson assembly NEBuilder HiFi DNA Assembly kit (New England Biolabs, Ipswich, MA, USA), adhering to the manufacturer's recommendations. In brief, synthetic DNAs (GeneArt, Thermo Fisher Scientific Inc., Rockford, IL, USA) were placed between the LCMV-GP and the VSV-L open reading frame of the VSV-GP vector backbone. Recombinant virus variants, expressing the additional gene that is not incorporated into the virion, were subsequently recovered by a helper virus-free calcium phosphate transfection in HEK293T cells using pCAG expression plasmids of T7 polymerase and VSV proteins N, P, and L, along with the respective virus construct that contained the VSV-GP vector.[46] Following detection of cytopathic effects and expansion on HEK293F cells, the virus progeny underwent two rounds of plaque purification and was further amplified on HEK293F cells.

### Separation method and orthogonal analytical methods

#### HPLC-SEC separation

An Acquity Arc Bio HPLC system equipped with a 2998-photodiode array (PDA) detector (Waters, Milford, MA, USA) and the software Empower 3 FR 5 (Waters, Milford, MA, USA) for data acquisition and integration was used in this work. The path length of the PDA flow cell was 10 mm. An MALS DAWN detector controlled by Astra 8.1 (Wyatt Technology, Santa Barbara, CA, USA) was integrated in the HPLC detector flow path. Analytical SEC column resins with mean pore sizes of 50 nm (TSKgel G4000PW) and >100 nm (TSKgel G6000PW) were used (Tosoh Bioscience, Griesheim, Germany). Column housings made of stainless-steel and PEEK (name affix "Bio-Assist") were tested during the method development. Tosoh uses an abbreviated term for the PEEK version of the G6000PW resin, which is "BioAssist G6PW". For more clarity, we refrain from using the abbreviated term. The PEEK version of the G4000PW was custom manufactured by Tosoh. A temperature-controlled column oven was used to keep the columns at 25°C during the method. The use of Waters Fraction Manager-Analytical (WFM-A) enabled the optional collection of elution fractions. The mobile phase used after screenings consisted of 50 mM Tris-HCl, 200 mM NaCl, 150 mM Arg, and 0.1 wt-% DMSO, pH 8.0, prepared with MilliQ purified water and 0.22 µm filtered (Corning, Glendale, AZ, USA). A constant flow rate of 0.5 mL/min was used, and the column was equilibrated for at least five column volumes before sample injections. A sample volume of 10 µL was used. For the CIP of the column, a high-salt buffer and a 20% methanol step were used.

#### Sample preparation

Samples were measured undiluted unless stated otherwise; if dilutions were required, a Tris-buffered, NaCl and 150 mM Arg-containing solution was used. A 50 g/L BSA stock solution was prepared from a lyophilized BSA heat shock fraction (Sigma-Aldrich, Saint-Louis, MO, USA) in a Tris-buffered, 50 mM NaCl-containing solution. The stock solution was used to spike 0.98 g/L BSA into each sample. Samples were then transferred to Quan Recovery polypropylene vials with a high-performance surface (Waters, Milford, MA, USA) and kept in the HPLC sample manager at 8°C until injection. Total Recovery glass vials (Waters, Milford, MA, USA) were also tested for comparison.

#### Separation characterization

The exclusion peak is presumed to be the virus peak. It was characterized by online UV and MALS signals and orthogonal offline analytical methods (described in following sections). Samples with and without BSA spikes were used to investigate the influence of BSA as the stabilizing agent on the exclusion peak. Virus variants of VSV-GP with increased genome length (up to 27%), resulting in prolonged VPs,[47] were used to evaluate the influence of different-sized VPs on the exclusion peak. Also, the MALS was used to acquire sizing data of the exclusion peak.

#### Ns-TEM quantification

Ns-TEM experiments were performed by NanoImaging Services (San Diego, CA, USA). VSV-GP containing samples were mixed 1:1 with 100 nm Polystyrene (PS) beads of predetermined concentration. The samples were transferred on a copper grid and stained using phosphotungstic acid. At least 50 images of different areas of

the grid containing sufficient amounts of PS beads and VPs were acquired at 15 000× magnification. Visible particles were classified into PS beads, bullet-shaped VPs, deformed VPs, and empty particles, and each class was counted. The particle concentration for each class is calculated based on the known PS bead concentration and the counted number $n$ for the virus particles $VP$ and $PS$ beads as shown in Equation 2. VP deformation can occur during the required sample treatment, which is why the sum of the bullet-shaped and deformed VPs class was used for subsequent calculations.

$$c(VP) = c(PS) * \frac{n(VP)}{n(PS)} \qquad \text{(Equation 2)}$$

### SDS-PAGE and silver staining

Collected SEC fractions were analyzed by SDS-PAGE (4%–20% Mini-PROTEAN TGX Precast Protein Gel; Bio-Rad, Hercules, CA, USA) and silver stained (Thermo Scientific Pierce Silver Stain Kit; Thermo Fisher Scientific Inc., Rockford, IL, USA), both methods were used according to the manufacturer's instructions.

### qPCR

Viral RNA was extracted using Ambion's MagMAX Viral RNA isolation kit (Life Technologies Corp., Carlsbad, CA, USA) according to the manufacturer's instruction. A CFX96 Real Time Cycler (Bio-Rad, Hercules, CA, USA) and iTaq Universal Probes One-Step Kit (Bio-Rad, Hercules, CA, USA) were used for qPCR analysis with primers targeting the N-protein gene sequences as described elsewhere.[48]

### TCID$_{50}$

BHK-21 cells (CLS Cell Lines Service GmbH, Eppelheim, Germany) were seeded in 96-well plates containing GMEM medium complemented with 10% fetal calf serum (FCS), 5% tryptose phosphate broth and 1% penicillin-streptomycin solution (all media components from Gibco, Thermo Fisher Scientific Inc., Rockford, IL, USA) and incubated at 37°C and 5% $CO_2$. 24 hours after seeding, a dilution series of the virus-containing samples was prepared. The complemented media is used to create half-$\log_{10}$ dilution steps that are then added individually to the seeded wells. The plates are incubated for 3 days and subsequently the confluence of each well is determined using an automated plate reader (Tecan, Männedorf, Switzerland). A confluence level of $\leq 95\%$ is used as a threshold to determine cytopathic effects in wells by virus infection. The TCID$_{50}$/mL is calculated based on the number of infected wells using the Spearman-Kärber equation.[49,50]

### Method development
### Recovery analysis

Quantifying analyte molecules by a post-column detector requires the targeted analyte to elute with a sufficiently high and reproducible recovery. Recovery was determined by comparing analyte injections over the column and PEEK bypass tubing. Five microliters of VSV-GP reference material and, as a model protein, 5 μL of 2 g/L BSA, were applied. The post-column and post-bypass UV 280 nm signal responses were compared, and recoveries calculated.

### Mobile phase screening

To improve the recovery of the SEC method, the mobile phase buffer was optimized. Various buffer components were screened: Tris, citrate, phosphate, NaCl, Arg, sorbitol, sucrose, and DMSO. Excipient concentrations as well as pH were optimized to reduce non-specific adsorption to the column resin. The initial buffer was based on Tris with NaCl and Arg at a pH of 7.5. A complete list of screened buffer compositions can be found in the supplement material, Table S1. The buffer components were iteratively optimized by single or combined adjustments of buffer components and additional additives. Buffer performance was evaluated by the above-described quantitative recovery analysis and the qualitative evaluation of the CIP peaks by the MALS detector.

### Sample stability optimization

The sample stability in the sample manager was evaluated using two different sample vial materials (glass and polypropylene) and a BSA-spiking methodology. VSV-GP reference samples were diluted to a concentration of $9 \times 10^9$ VP/mL and prepared with different BSA spike concentrations. Over a time frame of 35 h, the prepared samples were stored in the sample manager at 8°C either in Quan Recovery polypropylene (Waters, Milford, MA, USA) or Total Recovery glass vials (Waters, Milford, MA, USA). During this time, samples were repeatedly drawn from the vials and analyzed by HPLC-SEC quantification.

### Method characterization

The reference material for method development was used to generate a calibration curve. Eight concentration levels in the range from the undiluted reference material to the LLOQ were evaluated. For the higher concentrated range, the undiluted material and two dilutions with the factor 1.5 were used. For the lower concentrated range, a five-step dilution series with the factor 3.0 starting from the undiluted material was used. HPLC-SEC analysis was conducted in triplicates for each concentration level as previously described. The triplicate measurements were repeated in three independent runs, resulting in nine measurement points per concentration level. Independent runs on different dates and using different buffer batches ensured the robustness of the calibration curve from random influences.

For the performance evaluation, quality control samples (QCs) at four concentration levels across the working range were specified: High, Mid, Low, and LLOQ concentration level. QCs were produced by dilution of the characterization reference material, aliquoted, and stored at $-80°C$ until usage. Every QC level was quantified by HPLC-SEC in three repetitions on five independent runs. The independent runs differed in date and mobile phase buffer batch. The performance runs were evaluated for precision and accuracy. The theoretical LOD and LLOQ were determined based on the baseline noise with an SN ratio of 3:1 and 10:1.

From a virus production run involving multiple DSP steps, IPCs were collected and frozen at −80°C until analysis. The VPs in these samples were first removed by 0.1 mm filtration (Whatman Anotop 10 Plus; Cytiva, Marlborough, MA, USA). Then, the reference virus material was spiked back into each sample. Finally, the samples were analyzed by HPLC-SEC quantification.

**Chromatographic step mass balance**

The VSV-GP particle quantification method described herein was applied to investigate an exemplary process development chromatography run for enveloped viruses. Clarified supernatant containing not only virus but also cell media components and cell-derived impurities was loaded on a monolithic CEX column (CIMmultus SO3 1.0 mL; Sartorius BIA Separations, Ajdovščina, Slovenia) in bind-and-elute mode. The flowthrough during sample loading and the wash phases were collected for analysis. A salt step was applied to elute bound VPs, and the peak was collected in fractions for offline quantification by HPLC-SEC and qPCR. A mass balance of the VP loading and eluting in the elution phases was conducted; 1 M NaOH + 2 M NaCl was used for the CIP step of the column as specified by the manufacturer.

## DATA AND CODE AVAILABILITY

All data used to evaluate the conclusions of the article are present in the paper and/or the supplementary material. ViraTherapeutics GmbH is unable to provide raw data, protocols, or additional datasets.

## SUPPLEMENTAL INFORMATION

Supplemental information can be found online at https://doi.org/10.1016/j.omtm.2024.101252.

## AUTHOR CONTRIBUTIONS

Conceptualization, A.S. and J.N.; Investigation A.S., I.B., F.M., and D.X.; Formal analysis A.S. and D.X.; Writing - original draft, A.S.; Writing – review and editing, all authors; Supervision J.N. and J.H.

## DECLARATION OF INTERESTS

The authors declare no competing interests.

## REFERENCES

1. Dunbar, C.E., High, K.A., Joung, J.K., Kohn, D.B., Ozawa, K., and Sadelain, M. (2018). Gene therapy comes of age. Science *359*, eaan4672. https://doi.org/10.1126/science.aan4672.

2. U.S. National Library of Medicine (2023). Oncolytic viruses in clinical trials, search terms: "gene therapies" AND "virus", and "oncolytic virus". clinicaltrials.gov.

3. Singh, N., and Heldt, C.L. (2022). Challenges in downstream purification of gene therapy viral vectors. Curr. Opin. Chem. Eng. *35*, 100780. https://doi.org/10.1016/j.coche.2021.100780.

4. McCarron, A., Donnelley, M., McIntyre, C., and Parsons, D. (2016). Challenges of up-scaling lentivirus production and processing. J. Biotechnol. *240*, 23–30. https://doi.org/10.1016/j.jbiotec.2016.10.016.

5. Moleirinho, M.G., Silva, R.J.S., Alves, P.M., Carrondo, M.J.T., and Peixoto, C. (2020). Current challenges in biotherapeutic particles manufacturing. Expet Opin. Biol. Ther. *20*, 451–465. https://doi.org/10.1080/14712598.2020.1693541.

6. Srivastava, A., Mallela, K.M.G., Deorkar, N., and Brophy, G. (2021). Manufacturing Challenges and Rational Formulation Development for AAV Viral Vectors. J. Pharmaceut. Sci. *110*, 2609–2624. https://doi.org/10.1016/j.xphs.2021.03.024.

7. Lothert, K., Eilts, F., and Wolff, M.W. (2022). Quantification methods for viruses and virus-like particles applied in biopharmaceutical production processes. Expert Rev. Vaccines *21*, 1029–1044. https://doi.org/10.1080/14760584.2022.2072302.

8. Parupudi, A., Gruia, F., Korman, S.A., Dragulin-Otto, S., Sra, K., Remmele, R.L., and Bee, J.S. (2017). Biophysical characterization of influenza A virions. J. Virol. Methods *247*, 91–98. https://doi.org/10.1016/j.jviromet.2017.06.002.

9. Heider, S., and Metzner, C. (2014). Quantitative real-time single particle analysis of virions. Virology *462–463*, 199–206. https://doi.org/10.1016/j.virol.2014.06.005.

10. Spitteler, M.A., Romo, A., Magi, N., Seo, M.-G., Yun, S.-J., Barroumeres, F., Régulier, E.G., and Bellinzoni, R. (2019). Validation of a high performance liquid chromatography method for quantitation of foot-and-mouth disease virus antigen in vaccines and vaccine manufacturing. Vaccine *37*, 5288–5296. https://doi.org/10.1016/j.vaccine.2019.07.051.

11. Chahal, P.S., Transfiguracion, J., Bernier, A., Voyer, R., Coffey, M., and Kamen, A. (2007). Validation of a high-performance liquid chromatographic assay for the quantification of Reovirus particles type 3. J. Pharm. Biomed. Anal. *45*, 417–421. https://doi.org/10.1016/j.jpba.2007.06.025.

12. van Tricht, E., Geurink, L., Backus, H., Germano, M., Somsen, G.W., and Sänger-van de Griend, C.E. (2017). One single, fast and robust capillary electrophoresis method for the direct quantification of intact adenovirus particles in upstream and downstream processing samples. Talanta *166*, 8–14. https://doi.org/10.1016/j.talanta.2017.01.013.

13. Transfiguracion, J., Tran, M.Y., Lanthier, S., Tremblay, S., Coulombe, N., Acchione, M., and Kamen, A.A. (2020). Rapid In-Process Monitoring of Lentiviral Vector Particles by High-Performance Liquid Chromatography. Mol. Ther. Methods Clin. Dev. *18*, 803–810. https://doi.org/10.1016/j.omtm.2020.08.005.

14. Transfiguracion, J., Coelho, H., and Kamen, A. (2004). High-performance liquid chromatographic total particles quantification of retroviral vectors pseudotyped with vesicular stomatitis virus-G glycoprotein. J. Chromatogr. B *813*, 167–173. https://doi.org/10.1016/j.jchromb.2004.09.034.

15. Steppert, P., Burgstaller, D., Klausberger, M., Tover, A., Berger, E., and Jungbauer, A. (2017). Quantification and characterization of virus-like particles by size-exclusion chromatography and nanoparticle tracking analysis. J. Chromatogr. A *1487*, 89–99. https://doi.org/10.1016/j.chroma.2016.12.085.

16. Pereira Aguilar, P., González-Domínguez, I., Schneider, T.A., Gòdia, F., Cervera, L., and Jungbauer, A. (2019). At-line multi-angle light scattering detector for faster process development in enveloped virus-like particle purification. J. Separ. Sci. *42*, 2640–2649. https://doi.org/10.1002/jssc.201900441.

17. Ge, P., Tsao, J., Schein, S., Green, T.J., Luo, M., and Zhou, Z.H. (2010). Cryo-EM Model of the Bullet-Shaped Vesicular Stomatitis Virus. Science *327*, 689–693. https://doi.org/10.1126/science.1181766.

18. Letchworth, G.J., Rodriguez, L.L., and del C Barrera, J. (1999). Vesicular Stomatitis. Vet. J. *157*, 239–260. https://doi.org/10.1053/tvjl.1998.0303.

19. Munis, A.M., Bentley, E.M., and Takeuchi, Y. (2020). A tool with many applications: vesicular stomatitis virus in research and medicine. Expet Opin. Biol. Ther. *20*, 1187–1201. https://doi.org/10.1080/14712598.2020.1787981.

20. Muik, A., Kneiske, I., Werbizki, M., Wilflingseder, D., Giroglou, T., Ebert, O., Kraft, A., Dietrich, U., Zimmer, G., Momma, S., and von Laer, D. (2011). Pseudotyping Vesicular Stomatitis Virus with Lymphocytic Choriomeningitis Virus Glycoproteins Enhances Infectivity for Glioma Cells and Minimizes Neurotropism. J. Virol. *85*, 5679–5684. https://doi.org/10.1128/jvi.02511-10.

21. Muik, A., Stubbert, L.J., Jahedi, R.Z., Geiβ, Y., Kimpel, J., Dold, C., Tober, R., Volk, A., Klein, S., Dietrich, U., et al. (2014). Re-engineering Vesicular Stomatitis Virus to Abrogate Neurotoxicity, Circumvent Humoral Immunity, and Enhance Oncolytic Potency. Cancer Res. 74, 3567–3578. https://doi.org/10.1158/0008-5472.can-13-3306.

22. Gélinas, J.F., Kiesslich, S., Gilbert, R., and Kamen, A.A. (2020). Titration methods for rVSV-based vaccine manufacturing. MethodsX 7, 100806. https://doi.org/10.1016/j.mex.2020.100806.

23. Abdelmageed, A.A., and Ferran, M.C. (2020). The Propagation, Quantification, and Storage of Vesicular Stomatitis Virus. Curr. Protoc. Microbiol. 58, e110. https://doi.org/10.1002/cpmc.110.

24. Hebert, C.G., DiNardo, N., Evans, Z.L., Hart, S.J., and Hachmann, A.-B. (2018). Rapid quantification of vesicular stomatitis virus in Vero cells using Laser Force Cytology. Vaccine 36, 6061–6069. https://doi.org/10.1016/j.vaccine.2018.09.002.

25. Akpinar, F., and Yin, J. (2015). Characterization of vesicular stomatitis virus populations by tunable resistive pulse sensing. J. Virol. Methods 218, 71–76. https://doi.org/10.1016/j.jviromet.2015.02.006.

26. Yang, L., and Yamamoto, T. (2016). Quantification of Virus Particles Using Nanopore-Based Resistive-Pulse Sensing Techniques. Front. Microbiol. 7, 1500. https://doi.org/10.3389/fmicb.2016.01500.

27. Malenovska, H. (2013). Virus quantitation by transmission electron microscopy, TCID50, and the role of timing virus harvesting: A case study of three animal viruses. J. Virol. Methods 191, 136–140. https://doi.org/10.1016/j.jviromet.2013.04.008.

28. McCormick, W., and Mermel, L.A. (2021). The basic reproductive number and particle-to-plaque ratio: comparison of these two parameters of viral infectivity. Virol. J. 18, 92–95. https://doi.org/10.1186/s12985-021-01566-4.

29. Arakawa, T., Ejima, D., Li, T., and Philo, J.S. (2010). The critical role of mobile phase composition in size exclusion chromatography of protein pharmaceuticals. J. Pharmaceut. Sci. 99, 1674–1692. https://doi.org/10.1002/jps.21974.

30. U.S. Food and Drug Administration (2018). Bioanalytical Method Validation: Guidance for Industry.

31. Lothert, K., and Wolff, M.W. (2023). Chromatographic Purification of Viruses: State of the Art and Current Trends. In Bioprocess and Analytics Development for Virus-Based Advanced Therapeutics and Medicinal Products (ATMPs), S. Gautam, A.I. Chiramel, and R. Pach, eds. (Springer), pp. 145–169. https://doi.org/10.1007/978-3-031-28489-2_7.

32. Porterfield, J.Z., Dhason, M.S., Loeb, D.D., Nassal, M., Stray, S.J., and Zlotnick, A. (2010). Full-Length Hepatitis B Virus Core Protein Packages Viral and Heterologous RNA with Similarly High Levels of Cooperativity. J. Virol. 84, 7174–7184. https://doi.org/10.1128/jvi.00586-10.

33. Vajda, J., Weber, D., Brekel, D., Hundt, B., and Müller, E. (2016). Size distribution analysis of influenza virus particles using size exclusion chromatography. J. Chromatogr. A 1465, 117–125. https://doi.org/10.1016/j.chroma.2016.08.056.

34. Makra, I., Terejánszky, P., and Gyurcsányi, R.E. (2015). A method based on light scattering to estimate the concentration of virus particles without the need for virus particle standards. MethodsX 2, 91–99. https://doi.org/10.1016/j.mex.2015.02.003.

35. Ejima, D., Yumioka, R., Arakawa, T., and Tsumoto, K. (2005). Arginine as an effective additive in gel permeation chromatography. J. Chromatogr. A 1094, 49–55. https://doi.org/10.1016/j.chroma.2005.07.086.

36. Wallis, C., and Melnick, J.L. (1968). Stabilization of enveloped viruses by dimethyl sulfoxide. J. Virol. 2, 953–954. https://doi.org/10.1128/jvi.2.9.953-954.1968.

37. Gordeliy, V.I., Kiselev, M.A., Lesieur, P., Pole, A.V., and Teixeira, J. (1998). Lipid Membrane Structure and Interactions in Dimethyl Sulfoxide/Water Mixtures. Biophys. J. 75, 2343–2351. https://doi.org/10.1016/s0006-3495(98)77678-7.

38. Marczewski, A.W. (2010). Analysis of Kinetic Langmuir Model. Part I: Integrated Kinetic Langmuir Equation (IKL): A New Complete Analytical Solution of the Langmuir Rate Equation. Langmuir 26, 15229–15238. https://doi.org/10.1021/la1010049.

39. Kovalchuk, S.I., Anikanov, N.A., Ivanova, O.M., Ziganshin, R.H., and Govorun, V.M. (2015). Bovine serum albumin as a universal suppressor of non-specific peptide binding in vials prior to nano-chromatography coupled mass-spectrometry analysis. Anal. Chim. Acta 893, 57–64. https://doi.org/10.1016/j.aca.2015.08.027.

40. Lorbetskie, B., Wang, J., Gravel, C., Allen, C., Walsh, M., Rinfret, A., Li, X., and Girard, M. (2011). Optimization and qualification of a quantitative reversed-phase HPLC method for hemagglutinin in influenza preparations and its comparative evaluation with biochemical assays. Vaccine 29, 3377–3389. https://doi.org/10.1016/j.vaccine.2011.02.090.

41. Transfiguracion, J., Manceur, A.P., Petiot, E., Thompson, C.M., and Kamen, A.A. (2015). Particle quantification of influenza viruses by high performance liquid chromatography. Vaccine 33, 78–84. https://doi.org/10.1016/j.vaccine.2014.11.027.

42. Murakami, P., and McCaman, M.T. (1999). Quantitation of Adenovirus DNA and Virus Particles with the PicoGreen Fluorescent Dye. Anal. Biochem. 274, 283–288. https://doi.org/10.1006/abio.1999.4282.

43. Transfiguracion, J., Mena, J.A., Aucoin, M.G., and Kamen, A.A. (2011). Development and validation of a HPLC method for the quantification of baculovirus particles. J. Chromatogr. B 879, 61–68. https://doi.org/10.1016/j.jchromb.2010.11.011.

44. Xia, Y.Q., Liu, D.Q., and Bakhtiar, R. (2002). Use of online-dual-column extraction in conjunction with chiral liquid chromatography tandem mass spectrometry for determination of terbutaline enantiomers in human plasma. Chirality 14, 742–749. https://doi.org/10.1002/chir.10135.

45. Mueller, D., Pardo Garcia, A., Grein, T.A., Kaess, F., Ng, J., Pesta, K., Schneider, S., and Turnbull, J. (2022). Process for Producing a Purified Rhabdovirus from Cell Culture. U.S. Patent No. US-20220010286-A1 1.

46. Heilmann, E., Kimpel, J., Geley, S., Naschberger, A., Urbiola, C., Nolden, T., von Laer, D., and Wollmann, G. (2019). The Methyltransferase Region of Vesicular Stomatitis Virus L Polymerase Is a Target Site for Functional Intramolecular Insertion. Viruses 11, 989. https://doi.org/10.3390/v11110989.

47. Soh, T.K., and Whelan, S.P.J. (2015). Tracking the Fate of Genetically Distinct Vesicular Stomatitis Virus Matrix Proteins Highlights the Role for Late Domains in Assembly. J. Virol. 89, 11750–11760. https://doi.org/10.1128/jvi.01371-15.

48. Wilmschen, S., Schneider, S., Peters, F., Bayer, L., Issmail, L., Bánki, Z., Grunwald, T., von Laer, D., and Kimpel, J. (2019). RSV Vaccine Based on Rhabdoviral Vector Protects after Single Immunization. Vaccines 7, 59. https://doi.org/10.3390/vaccines7030059.

49. Kärber, G. (1931). Beitrag zur kollektiven Behandlung pharmakologischer Reihenversuche. Archiv f. experiment. Pathol. u. Pharmakol. 162, 480–483. https://doi.org/10.1007/bf01863914.

50. Spearman, C. (1908). The method of "right and wrong cases" ('constant stimuli') without Gauss formulae. Br. J. Psychol. 2, 227–242. https://doi.org/10.1111/j.2044-8295.1908.tb00176.x.